

CD133/CD140a-Based Isolation of Distinct Human Multipotent Neural Progenitor Cells and Oligodendrocyte Progenitor Cells

Jing Wang, Melanie A. O'Bara, Suyog U. Pol, and Fraser J. Sim

The mechanisms underlying the specification of oligodendrocyte fate from multipotent neural progenitor cells (NPCs) in developing human brain are unknown. In this study, we sought to identify antigens sufficient to distinguish NPCs free from oligodendrocyte progenitor cells (OPCs). We investigated the potential overlap of NPC and OPC antigens using multicolor fluorescence-activated cell sorting (FACS) for CD133/PROM1, A2B5, and CD140a/PDGFR antigens. Surprisingly, we found that CD133, but not A2B5, was capable of enriching for OLIG2 expression, *Sox10* enhancer activity, and oligodendrocyte potential. As a subpopulation of CD133-positive cells expressed CD140a, we asked whether CD133 enriched *bone fide* NPCs regardless of CD140a expression. We found that CD133⁺CD140a⁻ cells were highly enriched for neurosphere initiating cells and were multipotent. Importantly, when analyzed immediately following isolation, CD133⁺CD140a⁻ NPCs lacked the capacity to generate oligodendrocytes. In contrast, CD133⁺CD140a⁺ cells were OLIG2-expressing OPCs capable of oligodendrocyte differentiation, but formed neurospheres with lower efficiency and were largely restricted to glial fate. Gene expression analysis further confirmed the stem cell nature of CD133⁺CD140a⁻ cells. As human CD133⁺ cells comprised both NPCs and OPCs, CD133 expression alone cannot be considered a specific marker of the stem cell phenotype, but rather comprises a heterogeneous mix of glial restricted as well as multipotent neural precursors. In contrast, CD133/CD140a-based FACS permits the separation of defined progenitor populations and the study of neural stem and oligodendrocyte fate specification in the human brain.

Introduction

THE DEVELOPMENT OF CELLULAR therapies for myelin replacement is reliant on the preparation of myelinogenic human cells with sufficient number and purity [1]. Although various fetal human preparations can mediate extensive myelination following engraftment into *shiverer/rag2* mice [2–4], primary fetal cells are limited by the quantity of appropriate tissue samples and/or require extensive expansion *in vitro* before transplantation. The influence of the *shiverer/rag2* environment on oligodendrocyte progenitor cell (OPC) specification and differentiation, and the applicability of these cell preparations for remyelination following acquired demyelination in adult CNS remain open questions. Although pluripotent stem cells represent a potentially unlimited supply of any somatic cell, the directed differentiation of human pluripotent cells toward oligodendrocyte fate currently relies on protracted culture techniques that are based on rodent development. As it is clear that human and mouse OPCs behave differently *in vitro* [5] and express overlapping yet divergent gene expression

profiles following isolation [6], rational approaches to direct oligodendrocyte specification will require a direct study of human OPC development.

A prerequisite for the molecular study of initial OPC specification in the human brain is the isolation of multipotent neural progenitor cells (NPCs) and neural stem cells in high purity, devoid of contaminating OPCs. We have previously shown that the A2B5 antigen overlaps with PDGFR/CD140a. Importantly, while A2B5⁺CD140a⁺ cells are capable of rapid oligodendrocyte differentiation, A2B5⁺CD140a⁻ do not acquire O4 antigen expression *in vitro* [7]. Likewise, we have observed that PROM1/CD133 mRNA expression was highly enriched in human CD140a-sorted fetal OPCs [7] and human A2B5-isolated adult OPCs [6] suggesting that CD133 may overlap with CD140a-defined OPCs as well as more primitive multipotent NPCs [8]. These data suggested that A2B5 or CD133 might be capable of enriching for CD140a/PDGFR negative stem/progenitor cells immediately before OPC commitment. Although various antigens can enrich NPCs, the extent of overlap with OPC expression was unknown. We hypothesized that

CD133⁺ or A2B5⁺ cells might be heterogeneous comprised of NPCs as well as already committed OPCs that coexpressed both CD133 and CD140a.

In this study, we used fluorescence-activated cell sorting (FACS) to determine an antigen combination capable of separating distinct populations of human NPCs from OPCs. We found that CD133 and not A2B5 antigen expression was capable of enriching for OLIG2-expressing progenitor cells in dissociates of the fetal human brain. CD133⁺ cells were themselves heterogeneous with respect to CD140a/PDGF α R antigenicity. CD133/CD140a-based FACS was sufficient to separate multipotent neurosphere-forming CD133⁺CD140a⁻ NPCs from CD133⁺CD140a⁺ OPCs capable of rapid oligodendrocyte differentiation. The differences in phenotypic behavior in vitro were reflected by the distinct transcription profiles of each subpopulation, which in turn, predicted the observed cellular phenotype. These transcriptomic analyses provide a valuable database for the identification of genes and cell signaling cascades specific to each cell type and means by which to influence oligodendrocyte fate in human neural precursors.

Materials and Methods

Tissue samples

Fetal brain samples of 15–22 weeks gestational age (g.a.) were obtained from patients who consented to tissue use under protocols approved by the local institutional review board. Dissociates were prepared and cultured in serum-free media (as detailed in [7]), with 10 ng/mL FGF2 (PeproTech).

Cytometry/FACS

Cytometry and sorting was performed using a BD FACSARIA (Becton Dickinson). For CD133/A2B5, cells were stained with CD133-APC (Miltenyi Biotec) and A2B5 IgM (Clone 105; ATCC), and goat anti-mouse IgM F(ab') PerCP (Jackson ImmunoResearch) or goat anti-mouse IgM A488 (Invitrogen). For CD133/CD140a, cells were stained with CD140a-PE (BD Pharmingen) and CD133-APC. Matched fluorescence minus-one controls were used to set gates following doublet discrimination. The incidence of CD133- and CD140a-positive cells was compared by one-way analysis of variance (ANOVA), followed by the Tukey's multiple comparison test (***) indicates $P < 0.001$ vs. CD133⁺CD140a⁻ cells). Typically from 10⁸ stained cells, we obtained between 0.5–1 $\times 10^6$ CD133⁺CD140a⁻ cells and $< 3 \times 10^5$ CD133⁺CD140a⁺ cells.

Immunocytochemistry and quantification

Twenty hours. Each cell population was seeded at 1×10^5 cells/mL into 48-well plates coated with poly-L-ornithine and laminin in SFM supplemented with the EGF (20 ng/mL) and FGF-2 (20 ng/mL). Cells were immunostained for mouse anti-CD140a (1:50; BD Pharmingen), mouse anti- β III tubulin/Tuj1 (1:1,000; Covance), and mouse anti-Nestin (1:1,000; Millipore). Alexa 594-, 647-, and 488-conjugated goat secondary antibodies were used at 1:500 (Invitrogen).

Four & eleven days. Cells were seeded at 5×10^4 /mL into 24-well plates coated with poly-L-ornithine and laminin in SFM lacking growth factors to promote differentiation. OLIG2/O4 immunocytochemistry was performed as de-

scribed in Conway et al. [9], additional staining was performed as described. The proportion of OLIG2 and O4-stained cells was quantified in 10 random fields at 200 \times magnification (Olympus IX51), representative of over 200 random cells. The proportion of cells was calculated for each tissue sample and the overall mean calculated ($n = 3$ –4, fetal tissue samples). In Fig. 1E, where the O4 frequency was less than 1%, every O4⁺ cell was counted and the proportion determined as a fraction of the cell plated. At each time point, statistical significance between sorted fractions was determined by one-way ANOVA, followed by the Tukey's multiple comparison test (GraphPad Prism 5.01).

Neurospheres. To permit adherence and differentiation, neurospheres were collected and seeded onto poly-L-ornithine/laminin-coated plates in SFM for 4 days. Following live O4 staining, cultures were washed, fixed, and immunostained for mouse anti- β III tubulin and mouse anti-GFAP (1:500; Sigma-Aldrich). In each cellular fraction, every plated sphere was classified on the basis of the differentiated progeny growing from the sphere [i.e., neuron (N), astrocyte (A), and oligodendrocyte (O)]. The numbers of lineage-defined spheres from each sample were averaged ($n = 6$ fetal tissue samples). Data were analyzed by one-way ANOVA, followed by the Dunnett's post hoc test.

Sox10-MCS5:GFP reporter

After FACS, cells were plated at 5×10^4 cells/mL on ornithine/laminin-coated plates in SFM with EGF/FGF2 (20 ng/mL; PeproTech). The next day, cells were infected with Sox10-MCS5:GFP reporter lentivirus at 1 multiplicity of infection [10]. Cytometry was performed 4 days later. Cells were gated using FSC/SSC and GFP expression measured.

Limiting dilution and neurosphere assays

After CD133/CD140a FACS, cells were resorted directly into 96-well plates using an automated cell deposition unit. Each population was seeded in triplicate at 1 – 5×10^4 /mL in SFM with EGF/FGF2 (20 ng/mL) or PDGF-AA/FGF2 (20 and 5 ng/mL, respectively). Cultures were maintained for up to 4 weeks, with factors added every other day and media replaced as needed. Sphere counts were made at 2 and 3 weeks postsort. All spheres were counted using a phase microscope and triplicates averaged from each fetal sample ($n = 6$, fetal brain preparations). The counts for CD133⁺CD140a⁻ cells at 5×10^4 cells/mL were excluded from analysis due to the high number of spheres that formed resulting in merging of individual spheres at 2 weeks. Linear regression was performed using a zero intercept constraint (GraphPad). To determine the influence of the growth factor on sphere generation, two-way ANOVA was performed followed by Bonferroni post hoc testing (GraphPad Prism).

Real-time RT-PCR analyses

RNA extraction, first-strand synthesis, and real-time PCR were performed as described in [9] primers: PDGFRA-for CCTGGTCTGTGTTGGTGATTG, PDGFRA-Rev ATACCTCGGTTTCTGTTTCCAAAT; PROM1-for CAGAGTACAACGCCAAACCA, PROM1-Rev AAATCACGATGAGGGTCAGC. Samples were run in duplicate and gene expression calculated by $\Delta\Delta C_t$ analysis using GAPDH as a reference. Statistical

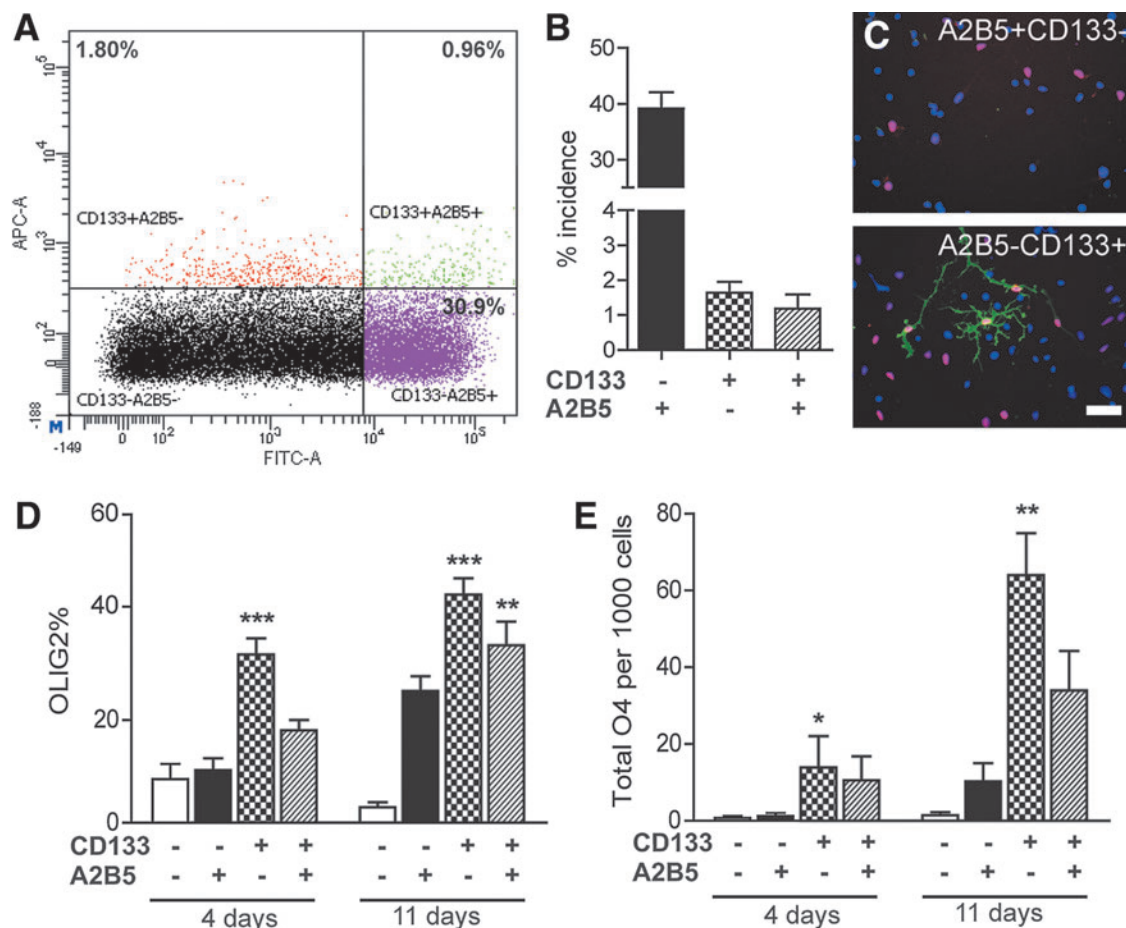


FIG. 1. CD133, not A2B5, differentially enriches for OLIG2 progenitor cells in the fetal human brain. **(A)** Two-color flow cytometry for CD133 (APC) and A2B5 (FITC) of 18 weeks gestational age (g.a.) fetal brain dissociate (30,000 events). **(B)** Mean \pm SEM% incidence of each fraction was quantified in 15–18 weeks g.a. samples ($n=5$ fetal brains). Following fluorescence-activated cell sorting (FACS), each fraction was immunostained for OLIG2 (red), O4 (green), and DAPI (blue) **(C)**, scale bar = 50 μ m, and OLIG2% quantified at 4 and 11 days postsort (mean \pm SEM, $n=4$ fetal samples). **(D)** One-way analysis of variance (ANOVA) at each time point; ** and *** indicate $P < 0.01$ and $P < 0.001$ versus CD133-A2B5 cells Tukey's post hoc test. **(E)** Oligodendrocyte lineage capacity was assessed using O4 immunocytochemistry and quantified (mean \pm SEM of total O4 cells from 25,000 cells plated, $n=3$ fetal samples). One-way ANOVA, * and ** indicate $P < 0.05$ and $P < 0.01$ versus CD133-A2B5 cells Tukey's post hoc test. Color images available online at www.liebertpub.com/scd

significance was determined by one-way ANOVA, followed by the Dunnett's post hoc test ($n=3$ fetal tissue samples).

Microarray analysis

RNA was amplified and Illumina HT-12v4 bead arrays analysis performed using R/Bioconductor as described in Conway et al. [9]. Gene set enrichment analysis (GSEA) was performed [11] using mSigDb [12], Biocarta, GO, and KEGG databases. The receiver operating characteristic (ROC)-based area under curve and significance of gene set enrichment were calculated according to *roc.area* [13]. Comparison between sorted cell populations was performed using the *roc.test* [14]. Receptor genes were defined as differentially expressed using a 10% false discovery rate and at least a threefold change ($n=3$, linear modeling empirical Bayes test statistic) [15]. The full analysis code is available on request (fjsim@buffalo.edu). The complete microarray data are available at NCBI GEO GSE40676 and may be browsed via the FINDb (www.FINDb.org).

Results

CD133, rather than A2B5, antigenicity enriches for OLIG2-expressing progenitor cells

As OLIG2 is expressed by multipotent NPCs [16] and OPCs before CD140a/PDGF α R [17,18], we first examined whether either A2B5 or CD133 was capable of enriching for OLIG2-expressing progenitors among fetal human brain dissociates. Flow cytometry revealed a large population of A2B5⁺ cells in human fetal brain dissociates ($40.3\% \pm 3.3\%$; $n=5$, 15–18 weeks g.a.) (Fig. 1A, B). In contrast, CD133 was relatively infrequent with $2.8\% \pm 0.71\%$, although similar to that previously described (3.6% [8]). We identified a subpopulation of CD133⁺A2B5⁺ cells, which represented $1.2\% \pm 0.4\%$ of the entire dissociate, and $39\% \pm 3.1\%$ of the CD133-defined population. Immunocytochemistry for OLIG2 revealed that $32.8\% \pm 3.2\%$ of CD133⁺A2B5⁻ cells expressed OLIG2 at 4 days in vitro ($n=4$, Fig. 1C, D). In contrast, both A2B5-expressing populations, CD133⁺A2B5⁺

and CD133⁺A2B5⁺, had a significantly lower OLIG2⁺ proportion ($18.0\% \pm 2.0\%$ and $10.3\% \pm 2.3\%$, respectively; one-way ANOVA, Tukey's post-test $P < 0.01$ vs. CD133⁺A2B5⁺). Importantly, the proportion of OLIG2⁺ cells was not enriched in either A2B5⁺ fraction relative to CD133⁺A2B5⁺ cells. Although OLIG2 expression is not limited to oligodendrocyte lineage cells [16], OLIG2 expression occurs in all OPCs; thus, the low frequency of OLIG2⁺ cells among A2B5⁺ cells indicates that A2B5 antigenicity did not significantly enrich for either population.

The high proportion of OLIG2-expressing precursors among the CD133⁺ fraction suggested that CD133 may be capable of enriching for early oligodendrocyte lineage cells. As such, we asked whether an OPC-specific *Sox10* enhancer might be differentially active between each fraction (Supplementary Fig. S1A, B; Supplementary Data are available online at www.liebertpub.com/scd). We previously found that *Sox10* enhancer cells, which drive high levels of GFP expression, GFP^{high}, express high levels of PDGFRA, OLIG2, and SOX10 mRNA indicative of OPC fate [10]. Although the incidence of GFP^{high} cells was relatively low ($< 25\%$) among CD133/A2B5 fractions, CD133⁺A2B5⁺ cells exhibited 3.3 ± 0.3 -fold higher mean GFP expression than CD133⁺A2B5⁺ cells and > 2 -fold higher GFP than CD133⁺A2B5⁺ cells ($n = 3$) (Supplementary Fig. S1C). This suggested that CD133⁺A2B5⁺ cells might contain a subpopulation in OPCs or represent a very early stage of oligodendrocytic commitment.

We therefore sought to determine the potential of CD133/A2B5-sorted cells to differentiate as oligodendrocytes. In comparison to CD140a-defined OPCs, which generate $> 30\%$ O4⁺ cells at 4 days [7], all CD133/A2B5-defined fractions generated very few oligodendrocytes ($< 2\%$ O4⁺ cells per 25,000 cells; $n = 4$; Fig. 1E). Although their potential for oligodendrocyte differentiation was limited, we noted that CD133⁺A2B5⁺ cells generated significantly more O4⁺ oligodendrocytes (23 ± 5 per 1,000 cells plated) than either CD133⁺A2B5⁺ or CD133⁺A2B5⁺ cells (0.97 ± 0.6 and 2.0 ± 0.6 O4⁺ cells, respectively; the Tukey's post-test $P < 0.05$; Fig. 1E). Unlike other fractions, the proportion of oligodendrocytes generated from CD133⁺A2B5⁺ cells increased with time, such that the O4% was significantly greater at 11 than 4 days suggesting progressive oligodendrocyte differentiation (two-way ANOVA, Bonferroni post-test $P < 0.01$; Fig. 1E). Thus, unlike A2B5, CD133 was capable of enriching for OLIG2-expressing progenitor with limited oligodendrocyte capacity. We next sought to determine the extent, if any, of antigenic overlap between CD133 and PDGF α R/CD140a populations.

CD140a-expressing CD133⁺ progenitors are oligodendrocyte progenitors in fetal human brain

Since PROM1 mRNA encoding CD133 was enriched in CD140a-sorted cells [7], we next asked whether CD133 and CD140a antigen expression overlapped in fetal dissociates. We hypothesized that CD140a expression among CD133⁺ cells might distinguish *bone fide* NPCs from more committed OPCs. Two-color cytometry revealed a substantial overlap of CD133 and CD140a, such that, $24\% \pm 3\%$ of CD133 cells expressed CD140a (mean \pm SEM, $n = 19$ fetal samples) (Fig. 2A, B). Likewise, over 50% of CD140a⁺ cells expressed CD133 ($52\% \pm 2\%$). To identify the initial phenotype of CD133/CD140a-sorted cells, we performed immunostaining 20 hours

postsort (Supplementary Fig. S2A–D). CD140a-sorted cells uniformly expressed CD140a/PDGF α R, while no CD140a labeling was observed in either CD133⁺CD140a⁺ cells or double-negative cells. We identified presumptive multipotent NPCs by nestin expression. No nestin⁺ cells were observed in the CD133⁺CD140a⁺ fraction and $\sim 5\%$ – 10% CD133⁺CD140a⁺ cells were nestin-expressing progenitors. Almost all double-negative cells expressed the neuronal marker Tuj1/ β III-tubulin with a only few nestin⁺ cells (less than 0.1%) (Supplementary Fig. S2A). In contrast, almost the entire CD133⁺CD140a⁺ fraction expressed high levels of nestin suggesting substantial enrichment of neural precursors specifically in the CD133⁺CD140a⁺ population (Supplementary Fig. S2B).

To determine their potential to generate oligodendrocytes in vitro, we maintained each fraction in pro-oligodendrocyte conditions for 4 days. As expected, very few OLIG2⁺ progenitors ($< 3\%$) or O4⁺ immature oligodendrocytes (0%) were observed in the double-negative population (Fig. 2C, G). Both CD140a⁺ fractions were highly enriched for OLIG2 progenitors with $78\% \pm 10\%$ from CD133⁺CD140a⁺ cells and $67\% \pm 7\%$ from CD133⁺CD140a⁺ cells ($n = 3$) (Fig. 2E–G). In contrast, $33\% \pm 4\%$ CD133⁺CD140a⁺ cells expressed OLIG2 (Fig. 2D, G). The proportion of OLIG2 cells could therefore be represented as CD140a⁺ $>$ CD133⁺CD140a⁺ $>$ CD133⁺CD140a⁺ (one-way ANOVA, Tukey's post-test; " $>$ " $P < 0.01$, " $>$ " $P < 0.05$). Both CD140a⁺ fractions rapidly gave rise to a substantial proportion of O4⁺ immature oligodendrocytes (Fig. 2E–G), while CD133⁺CD140a⁺ gave rise to $< 2\%$ O4 at 4 days ($1.1\% \pm 0.5\%$, $n = 3$ fetal samples) (Fig. 2D, G). As few CD133⁺CD140a⁺ and CD133⁺CD140a⁺ cells gave rise to oligodendrocytes, we examined these cultures for the presence of neuronal and astroglial differentiation (Supplementary Fig. S2E–H). The majority of double-negative CD133⁺CD140a⁺ cells remained as immature neurons and we noted occasional GFAP⁺ astrocytes. A substantial fraction of CD133⁺CD140a⁺ cells weakly expressed neuronal β III-tubulin, although several cells did not label with either neuronal or astrocytic antigens suggesting a more primitive phenotype.

As CD133⁺CD140a⁺ cells did not differentiate as oligodendrocytes, but expressed OLIG2, we sought to determine whether CD133⁺CD140a⁺ activated the *Sox10*-MCS5 enhancer. CD140a⁺ OPCs rapidly expressed *Sox10*-dependent GFP. By 4 days, a large fraction of CD140a⁺ cells expressed high levels of GFP (GFP^{high}) and those few cells, which did not typically exhibited a flatter morphology (Fig. 2I). In contrast, CD133⁺CD140a⁺ cells expressed GFP at lower levels (Fig. 2H). We used flow cytometry to quantify these differences (Fig. 2J, K). In comparison to CD140a-sorted OPCs, CD133⁺CD140a⁺ cells exhibited significantly lower median GFP expression (2.7 ± 0.3 -fold, $n = 3$ fetal samples). This was reflected by a significantly lower GFP^{high} percentage among CD133⁺CD140a⁺ compared to CD140a⁺ cells ($30.7\% \pm 1.8\%$ vs. $69.0\% \pm 7.5\%$, t -test $P = 0.0025$), suggesting that the *Sox10* enhancer activity correlated with OLIG2 expression in both fractions. Thus, by sorting with CD133 and CD140a together, we were able to distinguish CD133⁺CD140a⁺ cells, which were almost devoid of rapid oligodendrocyte differentiation and exhibited a reduced *Sox10* enhancer activity, from CD133⁺CD140a⁺ cells, which behaved as prototypic OPCs.

CD133⁺CD140a⁻ cells are enriched for neurosphere-forming multipotent progenitors

As CD133⁺ cells are typically considered as neural stem/progenitors [8], we next asked whether CD133/CD140a FACS might identify distinct fractions with respect to neurosphere initiation and multipotentiality. Sorted cells were directly seeded by secondary FACS at clonal densities be-

tween $1\text{--}5 \times 10^4/\text{mL}$ and maintained in the EGF/FGF. CD133⁺CD140a⁻ cells gave rise to large neurospheres (Fig. 3A, B). In contrast, CD133⁺CD140a⁺ cells gave rise to fewer and smaller neurospheres at each density (Fig. 3C, D). Both CD133-negative fractions generated even fewer neurospheres (data not shown). For example, when seeded at an initial density of 3×10^4 cells/mL, the mean number of neurospheres generated from CD133⁺CD140a⁻ cells was 47.21 ± 7.2 per 10^3 cells ($n=6$ fetal samples, 2 weeks in vitro, Fig. 3E). Both CD140a⁺ populations generated significantly fewer spheres compared to CD133⁺CD140a⁻ cells, 26.6 ± 3.8 and 19.1 ± 4.2 per 10^3 CD133⁺CD140a⁺ and CD133⁻CD140a⁺ plated cells, respectively ($P<0.01$, repeated measures one-way ANOVA, Tukey's post-test). The incidence of neurosphere-initiating cells (NS-IC) was calculated by linear regression across each density; CD133⁺CD140a⁻ (NS-IC activity 1/21 cells) \gg CD133⁺CD140a⁺ (1/35) \gg CD133⁻CD140a⁻ cells (one-way ANOVA, Tukey's post-test, $\gg \gg = P<0.001$). Thus, consistent with a NPC population, CD133⁺CD140a⁻ cells possessed a significantly greater NS-IC activity than other populations, while CD133⁺CD140a⁺ cells resembled a progenitor population with more limited NS-IC. Importantly, the frequency of the NS-IC activity in the CD133⁺CD140a⁻ population (1/21 cells) was much higher than previously reported among CD133⁺CD34⁻CD45⁻ cells (1/35 cells) suggesting that depletion of CD140a⁺ OPCs lead to a further enrichment of stem cells [8].

As sphere generation might be delayed in CD140a⁺ fractions, we also examined the NS-IC activity at 3 weeks and found similar results (data not shown). Furthermore, as CD140a⁺ cells express PDGF α R, we asked whether PDGF-AA supplementation might differentially support sphere generation. All CD133/CD140a populations, including CD133⁻CD140a⁺ and CD133⁺CD140a⁺ cells, generated fewer neurospheres when grown in PDGF/FGF (Fig. 3F). The relative decline in the NS-IC activity was greatest in CD140a⁺ populations (2.5 \times lower for CD140a⁺ fractions vs. 18% lower for CD133⁺CD140a⁻ cells).

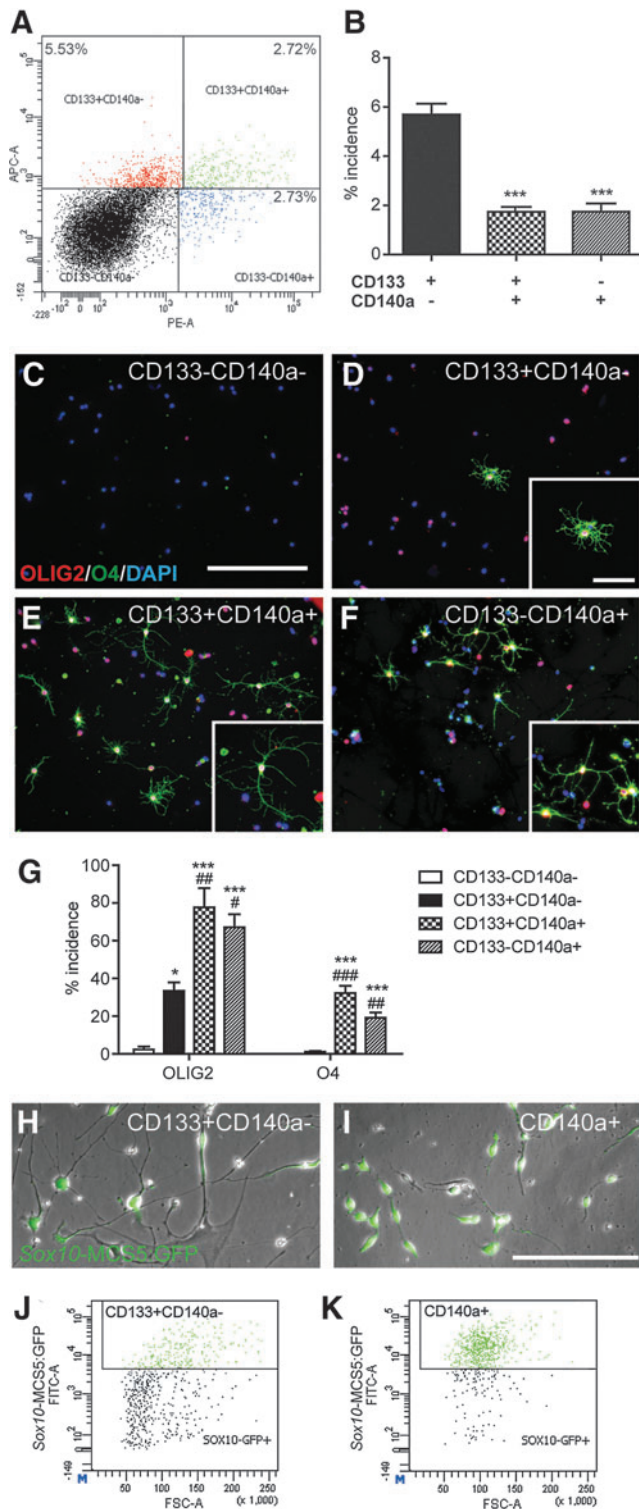
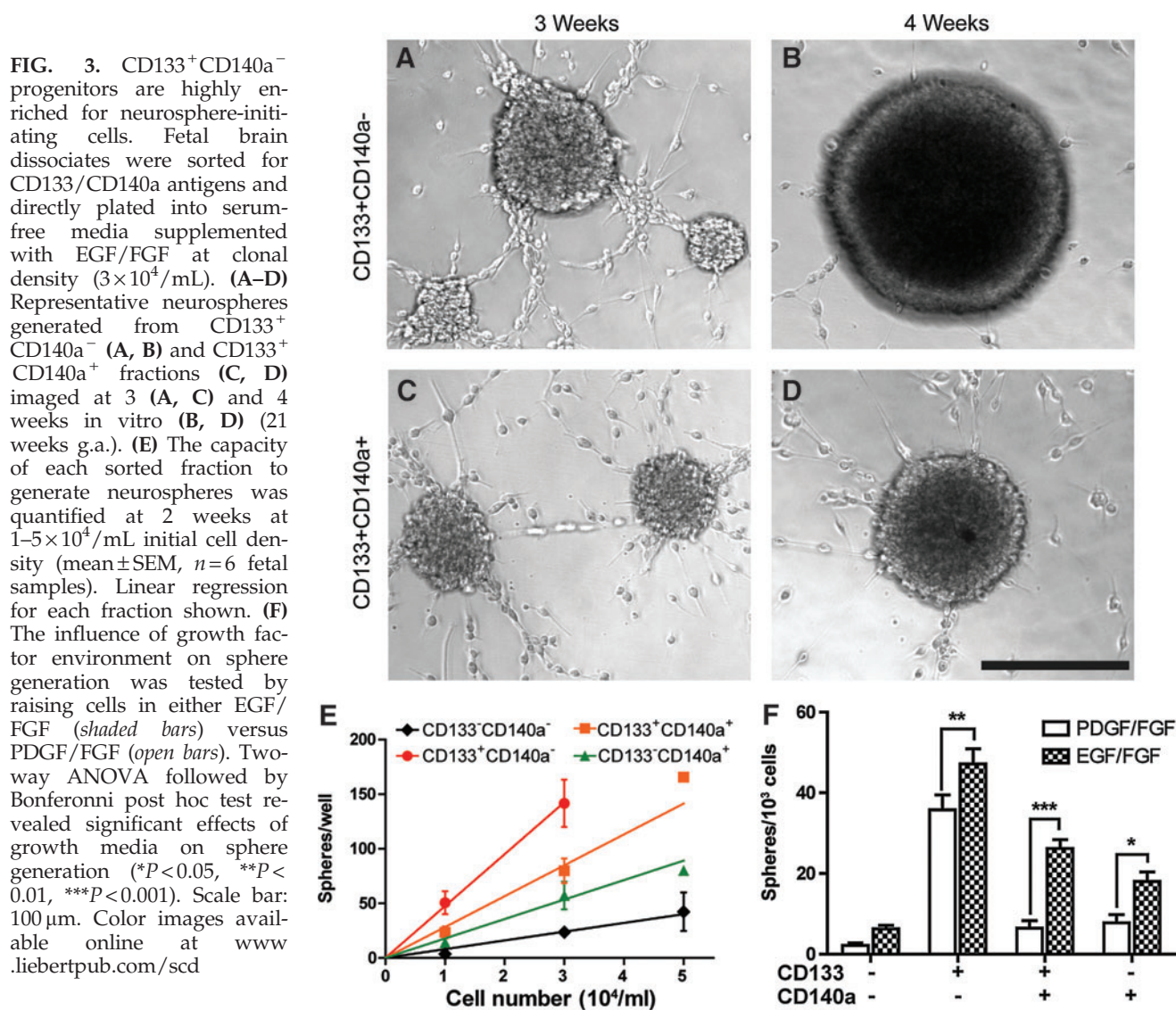


FIG. 2. CD140a defines an oligodendrocyte progenitor cell subpopulation of CD133⁺ neural progenitors. **(A)** Flow cytometry for CD133 (APC, y-axis) and CD140a (PE, x-axis) antigens reveals a population of CD133⁺CD140a⁺ cells in 20 weeks g.a. fetal human brain dissociates (30,000 events). **(B)** Mean \pm SEM percentage incidence of each fraction was quantified in 19–21 weeks g.a. samples ($n=19$ fetal brains). *** Indicates $P<0.001$ compared to CD133⁺CD140a⁻ (one-way ANOVA, Tukey's post hoc). **(C–F)** Immediately following FACS, each fraction was cultured in pro-oligodendrocyte conditions for 4 days and immunostained for OLIG2 (red), O4 (green), and DAPI (blue). Scale bar: 200 μ m (insets 60 μ m). **(G)** Quantification of oligodendrocyte lineage (OLIG2) and immature oligodendrocyte (O4) revealed significant difference between each fraction (mean \pm SEM; $n=4$ fetal samples, one-way ANOVA, Tukey's post hoc tests: * and *** indicate $P<0.05$ and $P<0.001$ respectively compared with CD133⁻CD140a⁻ cells; #, ##, and ### indicate $P<0.05$, $P<0.01$, and $P<0.001$, respectively, versus CD133⁺CD140a⁻ cells). **(H, I)** Sorted cells were infected with Sox10-MCS5:GFP lentivirus 1 day following isolation (4 days in vitro). Scale bar: 100 μ m. **(J, K)** Flow cytometry revealed a large difference in the activity of the Sox10 enhancer between CD133⁺CD140a⁻ cells (**J**) and CD140a⁺ cells (**K**) (4,000 events). Color images available online at www.liebertpub.com/scd



Thus, relative neurosphere formation was not differentially affected by these two media conditions.

CD133⁺CD140a⁻ cells are tripotential neural stem/progenitors, while CD133⁺CD140a⁺ are OPCs

To determine whether individual cells were multipotent, we plated EGF/FGF-expanded spheres into conditions favoring differentiation for 4 days and immunostained for markers of neuronal and glial lineage (Fig. 4A–D). Although multipotent or trilineage spheres containing neurons, astrocytes, and oligodendrocytes were found in each fraction, their frequency varied considerably (Fig. 4E). We found that $81\% \pm 2.6\%$ CD133⁺CD140a⁻ neurospheres were trilineage (mean \pm SEM, $n=6$). The absolute number and proportion of trilineage spheres in both CD140a⁺ fractions were significantly lower (Fig. 4E, one-way ANOVA, Tukey's post-test $P < 0.01$). In contrast, a larger proportion of CD140a⁺ spheres were solely glial composed, differentiating into oligodendrocytes and astrocytes (Fig. 4E). We also noted that the number of oligodendrocytes per sphere was greatest from CD140a⁺ cell-derived neurospheres. The neurosphere-like

clusters derived from CD133⁻CD140a⁻ cells typically generated only astrocytes (Fig. 4E). Spheres containing only neurons or oligodendrocytes were not observed in any fraction. As specific growth factor-derived signaling might alter the multipotentiality of cells in the neurosphere assay, we assessed cell fate following expansion of cells in PDGF-AA/FGF-2 supplemented media. Altering media conditions did not influence CD140a⁺-derived sphere lineage, but reduced the multilineage capacity of CD133⁺CD140a⁻ cells ($54\% \pm 2.9\%$, and data not shown). These data indicate that CD133/CD140a-based FACS was capable of separating distinct populations of CD133⁺CD140a⁻ NPCs from more committed CD140a⁺ OPCs.

CD133⁺CD140a⁻ multipotent progenitors were transcriptionally distinct from CD133⁺CD140a⁺ OPCs

As CD140a antigenicity distinguished phenotypically different subpopulations of CD133-sorted cells, we next asked whether initial transcriptional differences might reflect and predict the cellular fate of each sorted cell fraction. Immediately, after CD133/CD140a-based FACS, RNA was

extracted and processed. We first validated the sorted RNA using real-time RT-PCR for sort markers PROM1 (encoding CD133) and PDGFRA (CD140a). PROM1/CD133 mRNA was significantly and over 10-fold higher in both CD133⁺ populations (42- and 92-fold in CD133⁺CD140a⁻ and CD133⁺CD140a⁺, respectively). Similarly, PDGFRA/CD140a mRNA was significantly higher by greater than 100-fold in CD140a⁺ cells (276- and 802-fold in CD133⁻CD140a⁺ and CD133⁺CD140a⁺, respectively) (Fig. 5A).

We established the transcriptional profile of each fraction using Illumina microarrays ($n=3$; 18–19 weeks g.a.; NCBI GEO GSE40676). Data exploration using principle component analysis revealed distinct profiles between each population at a genome-wide scale (10,910 unique genes examined; Fig. 5B). On an individual transcript level, we examined the expression of known marker genes whose expression is relatively restricted to specific cell types (Fig.

5C). As expected, the multipotent CD133⁺CD140a⁻ cell fraction expressed high levels of known neural progenitor/stem cell genes such as nestin and SOX2/3. In contrast, OPC and oligodendrocyte lineage gene expression was restricted to both CD140a⁺ fractions. Neuronal transcripts were largely depleted from all sorted fractions relative to double-negative cells consistent with the frequency of Tuj1⁺ neurons observed immediately postsort (Supplementary Fig. S2).

However, as individual genes may be expressed by multiple cell lineages, we extended these analysis by performing GSEA against several large databases (Broad mSigDb, BioCarta, KEGG, GO) as well as our own database of >70 gene sets identified from relevant glial literature. Parametric GSEA of Broad mSigDB_C2 database revealed that >500 gene sets were differentially enriched between multipotent CD133⁺CD140a⁻ progenitors and both double-negative and CD133⁻CD140a⁺ OPCs [$<5\%$ false discovery rate (FDR)].

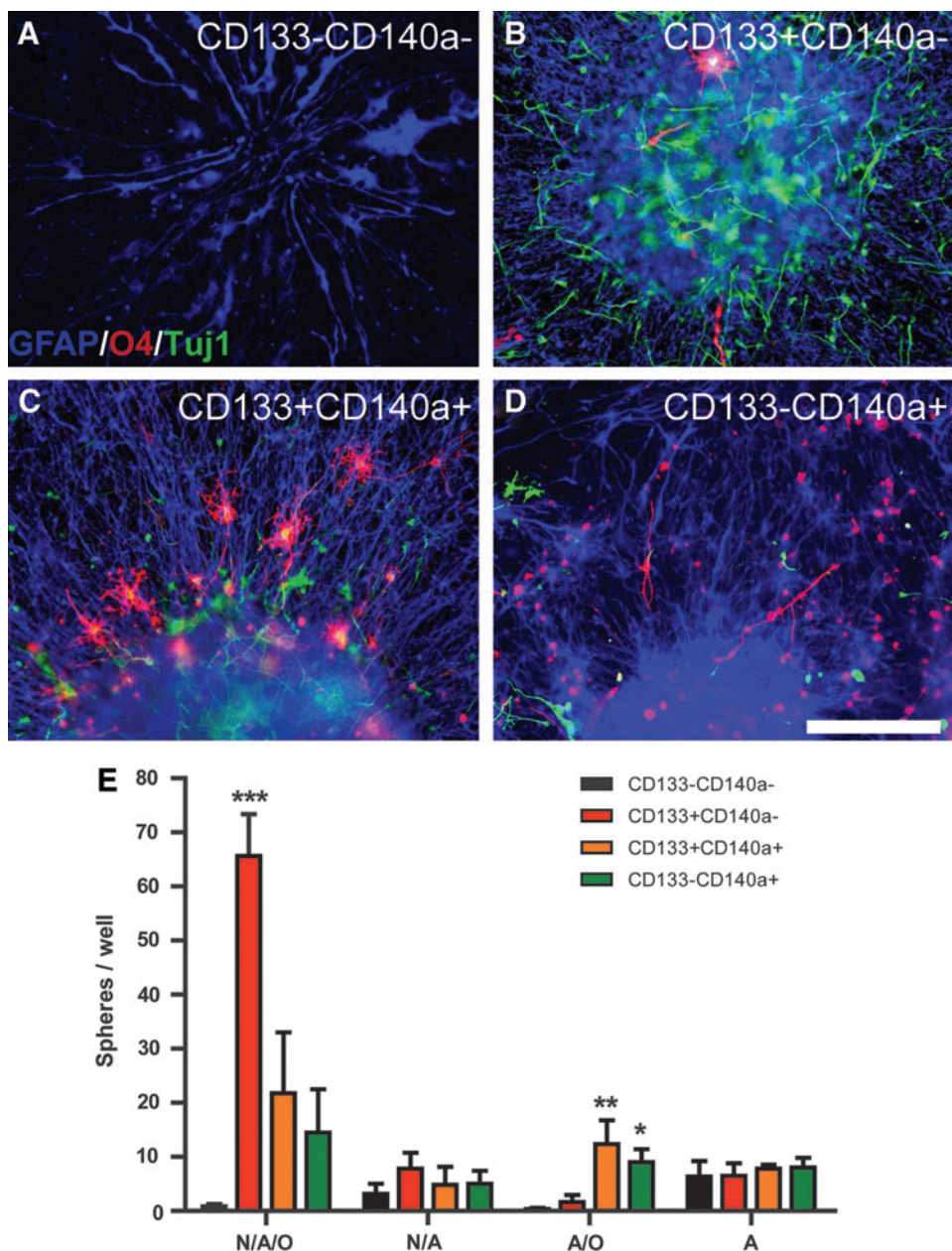
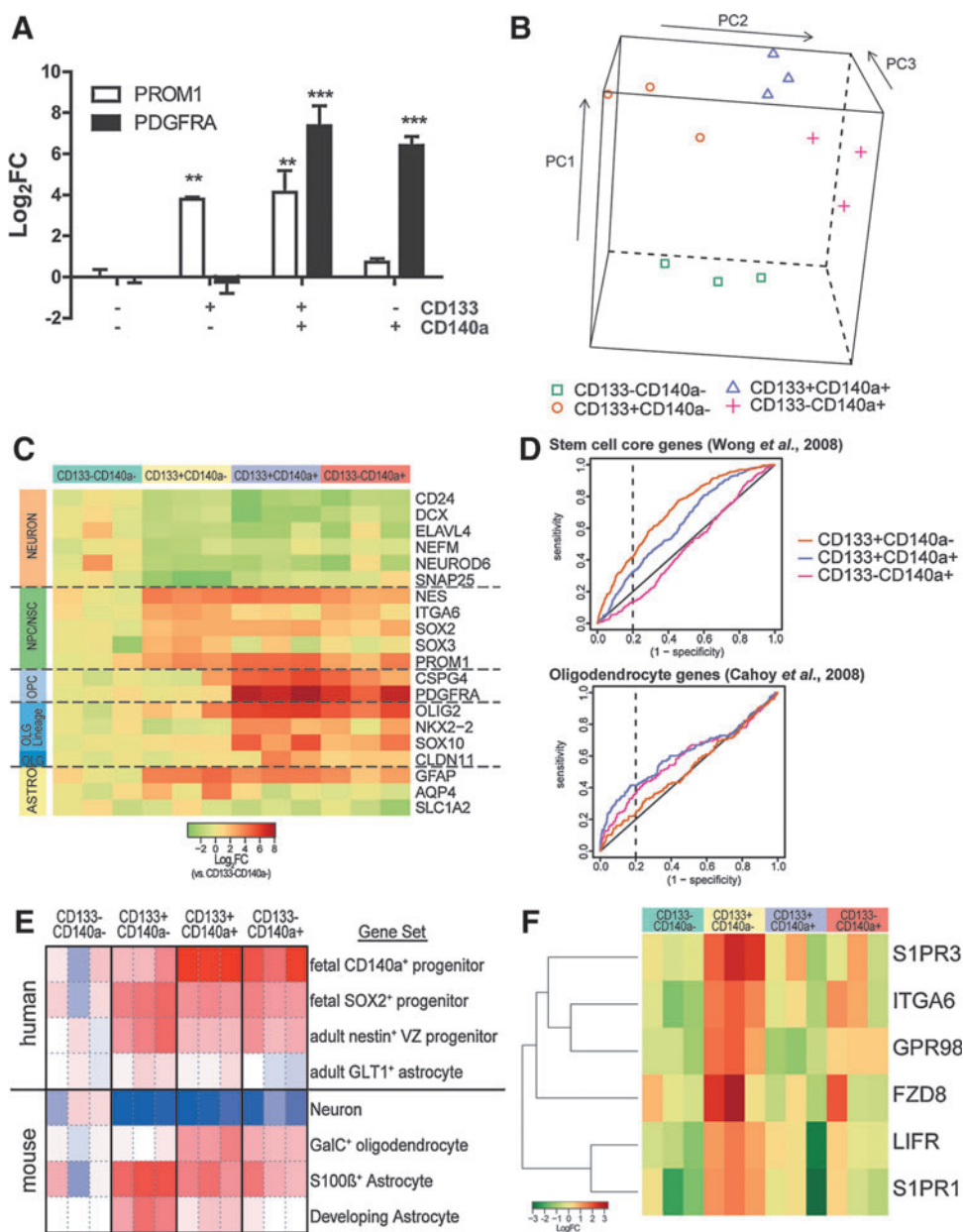


FIG. 4. CD133⁺CD140a⁻ antigenically defines multipotential neural stem/progenitor cells. (A–D) The lineage potential of each fraction was determined by plating spheres into prodifferentiation conditions and immunostaining for markers of neuron (β III-tubulin/Tuj1, green), astrocyte (GFAP, blue), and oligodendrocyte cells (O4, red). Scale bar = 200 μ m. (E) The number of spheres containing all three lineages (N/A/O), neurons/astrocytes (N/A), only glial lineages (A/O) or only astrocytes (A) were quantified (mean \pm SEM, $n=6$ fetal samples). *, **, and *** indicate Dunnett's post hoc $P < 0.05$, $P < 0.01$, and $P < 0.001$, respectively, compared with CD133⁻CD140a⁻. Color images available online at www.liebertpub.com/scd

FIG. 5. Transcriptional profiles of CD133⁺/CD140a⁺-defined progenitors. Human fetal brain dissociates were sorted for CD133⁺/CD140a⁺ and RNA immediately extracted. **(A)** Real-time RT-PCR for PROM1/CD133 and PDGFRA/CD140a mRNAs (mean log₂-fold change \pm SEM vs. CD133⁺CD140a⁺ cells, 18–19 weeks g.a.; $n=3$). Dunnett's post-test: ** $P<0.01$, *** $P<0.001$. **(B)** Principle component analysis. **(C)** Cell type-specific marker gene expression (heatmap: red and green indicate increased and decreased expression vs. median CD133⁺CD140a⁺). **(D)** Receiver operating characteristic analysis of stem cell core genes [19] and oligodendrocyte-expressed genes [22] in each sorted cell profile. The relative deflection above the line of identity (black) indicates enrichment of genes versus CD133⁺CD140a⁺ cells. **(E)** Gene set enrichment analysis (GSEA) was performed using cell type-specific gene expression profiles obtained from human (upper panel) and mouse (lower panel) sorted cells. The relative enrichment in each sorted RNA sample was visualized using a heatmap; red indicates relative enrichment to CD133⁺CD140a⁺ cells, and blue depletion. **(F)** Receptor genes selectively enriched in CD133⁺CD140a⁺ cells relative to both CD133⁺CD140a⁺ and CD133⁺CD140a⁺ cells. Color images available online at www.liebertpub.com/scd



Among them, a core stem cell module was significantly enriched (FDR q -value = 7.8×10^{-6}) [19]. Further, ROC analysis confirmed that core stem cell genes were highly enriched in CD133⁺CD140a⁺ cells relative to double-negative cells [area under the curve (AUC) = 0.71, P value = 4.62×10^{-34}], and, importantly, differentially enriched relative to CD133⁺CD140a⁺ OPCs (P value = 1.03×10^{-11}) (Fig. 5D). Embryonic, neural, and hematopoietic stem cell expressed genes were also highly enriched in CD133⁺CD140a⁺ cells (AUC comparison, P value = 4.9×10^{-5} and 2.5×10^{-10} relative to CD133⁺CD140a⁺ and CD133⁺CD140a⁺ cells, respectively) [20]. Likewise, stem cell depleted genes were enriched in CD140a⁺ cells (AUC P value = 1.6×10^{-4} and 1.5×10^{-5}). CD133⁺CD140a⁺ cells were also enriched in genes involved in telomere maintenance ($P = 2.9 \times 10^{-5}$ and 1.2×10^{-8}). Cell proliferation gene sets were similarly regulated between CD133⁺CD140a⁺ cells and both CD140a⁺ populations

($P = 7.6 \times 10^{-18}$ and 1.4×10^{-30} ; cycling genes in Ben-Porath et al. [21], and $P = 7.6 \times 10^{-18}$ and 1.7×10^{-43} ; cell cycle, Mitotic genes in Reactome.org). Taken together, the gene expression profile of CD133⁺CD140a⁺ cells was highly consistent with a neural stem/progenitor population and highly enriched for these traits relative to CD140a⁺ cells.

In contrast, among gene sets enriched in CD133⁺CD140a⁺ cells, we noted that adult human OPC-specific genes were highly enriched (AUC, $P = 7.8 \times 10^{-19}$) [6]. We also found significant enrichment of mouse oligodendrocyte expressed genes ($P = 0.00013$) [22] (Fig. 5D). We performed GSEA using a focused database of human and mouse sorted cells to better define the transcription differences between CD133⁺CD140a⁺ presumptive NPCs and double-positive CD133⁺CD140a⁺ OPC-like cells (Fig. 5E, upper panel). As expected, double-positive cells were highly enriched in genes previously identified using CD140a⁺ FACS and Affymetrix rather

than Illumina arrays ($P=2.9 \times 10^{-7}$) [7]. Interestingly, genes specifically expressed by *Sox2* enhancer-defined progenitors were not differentially enriched in either CD133⁺ fraction suggesting that like CD133, the *Sox2* enhancer activity was unable to distinguish NPC from OPC fate [23]. In contrast, nestin-expressing NPCs isolated from adult human VZ expressed a gene set that was differentially active in CD133⁺CD140a⁻ relative to CD133⁺CD140a⁺ cells ($P=8.7 \times 10^{-3}$) [24]. We next asked whether gene expression was conserved between species. GSEA revealed that mouse GalC⁺ oligodendrocyte genes were differentially enriched in CD140a⁺ cells and not enriched in CD133⁺CD140a⁻ cells (Fig. 5E, lower panel). In contrast, CD133⁺CD140a⁻ cells were relatively enriched in astrocyte-expressed genes, especially those identified as expressed by developing astrocytes (Table S15 in [22]). Consistent with our individual marker gene analysis and immunostaining, neuronal transcripts were depleted in all sorted fractions relative to double-negative cells.

To determine the specific receptors that were differentially expressed between cell fractions, we performed differential gene expression analysis. CD133⁺CD140a⁻ NPCs expressed six receptors greater than OPC and the double-negative populations (GO:0004872) (Fig. 5F). All of these receptors genes have been identified in the developing CNS and some have identified roles in NPC regulation [25–28]. As such, these receptors may provide specific means to target human multipotent NPCs.

Discussion

In this study, we sought to identify and separate distinct populations of NPCs and OPCs to permit a molecular understanding of the signaling cascades that regulate initial oligodendrocyte lineage specification. We initially asked whether CD133 or A2B5 antigens were capable of identifying neural progenitors that expressed OLIG2. Although OLIG2 can be expressed by multipotent NPCs in addition to the oligodendrocyte lineage [16], OLIG2 expression is maintained by oligodendrocytic cells and, as such, enrichment of OLIG2⁺ marker expression would accompany identification of early OPCs and oligodendrocyte lineage cells. Surprisingly, A2B5 antigenicity did not enrich for OLIG2⁺ cells relative to other CD133/A2B5-sorted fractions. In agreement with this observation, Cui and colleagues have reported a similarly low incidence of OLIG2-expressing cells following initial A2B5-based isolation and after 4 days in vitro [29]. Thus, as all OPCs are thought to express OLIG2, only a small subfraction of A2B5⁺ cells are of the oligodendrocyte lineage in the human fetal forebrain. As such, the utility of A2B5 sorting for molecular studies of human OPC development is limited. In contrast, we found that CD133-based sorting enriched for OLIG2⁺ cells, exhibited a greater *Sox10* enhancer activity, and possessed a limited, but nevertheless, significantly enriched capacity to generate oligodendrocytes in vitro compared to other fractions. As PROM1/CD133 was enriched in both adult and fetal human OPCs [6,7], we tested whether CD133 colocalized with CD140a⁺ OPCs in fetal dissociates. Two-color FACS revealed a significant overlap with approximately half of CD140a⁺ OPCs expressing CD133.

Interestingly, CD140a⁺ cells behaved as OPCs regardless of CD133 antigen status, retaining the capacity to rapidly differentiate as oligodendrocytes following isolation. Similar

to adult human OPCs [30], both CD140a⁺-defined populations exhibited a limited capacity for trilineage differentiation and NS-IC activity. The activation of PDGF α R via supplementation with PDGF-AA instead of EGF did not increase sphere formation nor promote multipotentiality. Indeed, the substitution of PDGF-AA for EGF reduced the NS-IC activity in both CD140a⁺ populations. Transcriptional analysis of CD133⁺CD140a⁺ and CD133⁻CD140a⁺ cells revealed significant commonality. These data indicate relatively minor phenotypic differences in CD133-defined subpopulations of CD140a⁺ cells and, as such, the subdivision of CD140a⁺ OPCs based on CD133 antigen expression is unlikely to yield significant benefits for cell therapy.

Importantly, CD140a⁺ antigenicity among CD133-defined cells was capable of distinguishing CD140a⁻ NPCs from CD140a⁺ OPCs. Although one third of CD133⁺CD140a⁻ cells expressed OLIG2, these cells lacked the capacity to generate significant numbers of O4⁺ oligodendrocytes. A smaller fraction of CD133⁺CD140a⁻ cells activated the *Sox10* enhancer and did not express OPC markers. The genomic comparison of CD133⁺CD140a⁻ NPCs to other fractions revealed enrichment for several gene sets associated with stem cells such as cell proliferation and telomere maintenance. The comparison to double-positive cells revealed that CD133⁺CD140a⁻ were highly enriched in adult human multipotent NPC-expressed genes [24]. As such, depletion of CD140a⁺ cells was sufficient to remove OPCs from the CD133⁺-defined pool. CD133⁺CD140a⁻ cells were capable of multilineage differentiation, exhibited a high NS-IC activity indicative of a neural precursor population, and expressed a gene signature enriched for known stem cell genes. Indeed, CD133⁺CD140a⁻ cells possessed a greater NS-IC activity compared to CD133 alone [8], integrin $\alpha 6/\beta 1$ [25], or *Sox2*-defined NPCs [23], and similar to CD133⁺CD24⁻ cells [8]. By removing OPCs from this pool, we have therefore defined a population of NPCs that may represent the immediate precursor to OPCs and permit the study of OPC commitment. This is an important step in the identification of small molecules for the induction of OPC fate from human fetal dissociates or pluripotent-derived cells.

CD133 antigenicity has been used to purify NPCs from human brain tissue for many years [8]. In this study, we found that CD133-expressing cells comprise a heterogeneous population of neural progenitors containing both CD140a⁻ multipotent NPCs and CD140a⁺ OPCs. This is important as the cellular fate and self-renewal potential are clearly distinct between these two fractions and their individual transcription profiles indicate divergent signaling cascades. The use of CD133 expression as a marker of NPC fate has become increasingly common, especially as a marker of tumor stem cells found in glioma and glioblastoma [31]. However, as CD133 also labels CD140a⁺ OPCs, normal adult OPCs express PROM1/CD133 [6], and OPCs represent a much larger mitotic population in the adult brain; it is likely that CD133 expression alone is not sufficient to determine NPC fate or derivation from glial neoplasms.

Finally, we have determined the transcriptional profile of each CD133/CD140a-defined population. As these represent distinct phenotypes of human NPCs and OPCs, this will likely permit the identification of novel pharmacological targets for induction of cell fate. It is important to emphasize that each sorted fraction likely remains heterogeneous, for

example, we know that roughly one third of CD133⁺CD140a⁻-defined NPCs express OLIG2. However, as this NPC fraction cannot rapidly differentiate as oligodendrocytes in vitro, the comparison of NPCs back to highly myelinogenic CD140a⁺ OPCs revealed several important molecular differences between the two populations. Indeed, the receptor analysis described herein accurately predicts several known receptors that may specifically regulate NPCs. For example integrin $\alpha 6$ (ITGA6) has been used as a cell-surface antigen to enrich for human NPCs [25]. LIFR mRNA expression is consistent with the fact that LIF has long been used as a NPC mitogen in human NPC culture [26]. Sphingosine 1-phosphate receptors (S1PR1 and S1PR3) have been described in human multipotent NPCs [32] and are thought to regulate migration, proliferation, and differentiation. GPR98 has been shown to be expressed in VZ during embryonic development [27] and is highly expressed in fetal human VZ during the second trimester (Sim, unpublished data). A role for GPR98 in multipotent NPC development has not yet been described. Finally, zebrafish frizzled 8 (FZD8) is required for oligodendrocyte development in the spinal cord as loss of Fz8a results in the failure to form both oligodendrocytes and OPCs [28]. Thus, each of the identified receptors identified in our genomic screen likely regulate NPCs and may therefore be targeted to identify a novel compound to induce OPC fate.

The genomic characterization and separation of NPCs and OPCs from the same tissue sample improves upon our previous genomic study of Sox2-defined precursors [23]. Our genomic analysis using GSEA provide evidence that Sox2-defined cells encompasses both NPCs and OPCs (similar to CD133 alone). Indeed, we noted that a subpopulation of CD140a-defined OPCs expressed the SOX2 protein before and after isolation [7]. As such, we would anticipate that the study of human OPC fate specification from CD133⁺CD140a⁻-defined NPCs will permit identification of treatments capable of directly influencing oligodendrocyte fate rather than merely selecting or expanding a subpopulation of OPCs already present in the larger population. This would be an important advance toward addressing the availability of suitable cells for myelinogenic cell therapy.

Acknowledgments

This work was supported, in part, by the Empire State Stem Cell Fund through New York State Department of Health Contracts C026413 and C026428. Opinions expressed here are solely those of the author and do not necessarily reflect those of the Empire State Stem Cell Board, the New York State Department of Health, or the State of New York. We thank Jeff Conroy of Roswell Park Cancer Institute for assistance with Illumina Beadarray techniques. We acknowledge the assistance of the Confocal Microscope and Flow Cytometry Facility in the School of Medicine and Biomedical Sciences, University at Buffalo. The microarray profiling was supported by grants from the National Institutes of Health/National Cancer Institute, P30 CA016056 (RPCI Cancer Center Support Grant).

Author Disclosure Statement

No competing financial interests exist.

References

1. Ben-Hur T. (2011). Cell therapy for multiple sclerosis. *Neurotherapeutics* 8:625–642.
2. Windrem MS, MC Nunes, WK Rashbaum, TH Schwartz, RA Goodman, G McKhann, 2nd, NS Roy and SA Goldman. (2004). Fetal and adult human oligodendrocyte progenitor cell isolates myelinate the congenitally dysmyelinated brain. *Nat Med* 10:93–97.
3. Windrem MS, SJ Schanz, M Guo, GF Tian, V Washco, N Stanwood, M Rasband, NS Roy, M Nedergaard, et al. (2008). Neonatal chimerization with human glial progenitor cells can both remyelinate and rescue the otherwise lethally hypomyelinated shiverer mouse. *Cell Stem Cell* 2:553–565.
4. Uchida N, K Chen, M Dohse, KD Hansen, J Dean, JR Buser, A Riddle, DJ Beardsley, Y Wan, et al. (2012). Human neural stem cells induce functional myelination in mice with severe dysmyelination. *Sci Transl Med* 4:155ra136.
5. Hu BY, ZW Du, XJ Li, M Ayala and SC Zhang. (2009). Human oligodendrocytes from embryonic stem cells: conserved SHH signaling networks and divergent FGF effects. *Development* 136:1443–1452.
6. Sim FJ, MS Windrem and SA Goldman. (2009). Fate determination of adult human glial progenitor cells. *Neuron Glia Biol* 5:45–55.
7. Sim FJ, CR McClain, SJ Schanz, TL Protack, MS Windrem and SA Goldman. (2011). CD140a identifies a population of highly myelinogenic, migration-competent and efficiently engrafting human oligodendrocyte progenitor cells. *Nat Biotechnol* 29:934–941.
8. Uchida N, DW Buck, D He, MJ Reitsma, M Masek, TV Phan, AS Tsukamoto, FH Gage and IL Weissman. (2000). Direct isolation of human central nervous system stem cells. *Proc Natl Acad Sci U S A* 97:14720–14725.
9. Conway GD, MA O'Bara, BH Vedia, SU Pol and FJ Sim. (2012). Histone deacetylase activity is required for human oligodendrocyte progenitor differentiation. *Glia* 60:1944–1953.
10. Pol S, J Lang, M O'Bara, T Cimato, A McCallion and F Sim. (2013). Sox10-MCS5 enhancer dynamically tracks human oligodendrocyte progenitor fate. *Exp Neurol* pii:S0014-4886(13)00093-9.
11. Furge KA, MH Tan, K Dykema, E Kort, W Stadler, X Yao, M Zhou and BT Teh. (2007). Identification of deregulated oncogenic pathways in renal cell carcinoma: an integrated oncogenomic approach based on gene expression profiling. *Oncogene* 26:1346–1350.
12. Subramanian A, P Tamayo, VK Mootha, S Mukherjee, BL Ebert, MA Gillette, A Paulovich, SL Pomeroy, TR Golub, ES Lander and JP Mesirov. (2005). Gene set enrichment analysis: a knowledge-based approach for interpreting genome-wide expression profiles. *Proc Natl Acad Sci U S A* 102:15545–15550.
13. Mason SJ and NE Graham. (2002). Areas beneath the relative operating characteristics (ROC) and relative operating levels (ROL) curves: statistical significance and interpretation. *Q J Roy Meteorol Soc* 128:2145–2166.
14. DeLong ER, DM DeLong and DL Clarke-Pearson. (1988). Comparing the areas under two or more correlated receiver operating characteristic curves: a nonparametric approach. *Biometrics* 44:837–845.
15. Smyth GK. (2004). Linear models and empirical bayes methods for assessing differential expression in microarray experiments. *Stat Appl Genet Mol Biol* 3:Article3.
16. Ligon KL, E Huillard, S Mehta, S Kesari, H Liu, JA Alberta, RM Bachoo, M Kane, DN Louis, et al. (2007). Olig2-regulated

- lineage-restricted pathway controls replication competence in neural stem cells and malignant glioma. *Neuron* 53: 503–517.
17. Lu QR, D Yuk, JA Alberta, Z Zhu, I Pawlitzky, J Chan, AP McMahon, CD Stiles and DH Rowitch. (2000). Sonic hedgehog—regulated oligodendrocyte lineage genes encoding bHLH proteins in the mammalian central nervous system. *Neuron* 25:317–329.
 18. Zhou Q, S Wang and DJ Anderson. (2000). Identification of a novel family of oligodendrocyte lineage-specific basic helix-loop-helix transcription factors. *Neuron* 25:331–343.
 19. Wong DJ, H Liu, TW Ridky, D Cassarino, E Segal and HY Chang. (2008). Module map of stem cell genes guides creation of epithelial cancer stem cells. *Cell Stem Cell* 2:333–344.
 20. Ramalho-Santos M, S Yoon, Y Matsuzaki, RC Mulligan and DA Melton. (2002). “Stemness”: transcriptional profiling of embryonic and adult stem cells. *Science* 298:597–600.
 21. Ben-Porath I, MW Thomson, VJ Carey, R Ge, GW Bell, A Regev and RA Weinberg. (2008). An embryonic stem cell-like gene expression signature in poorly differentiated aggressive human tumors. *Nat Genet* 40:499–507.
 22. Cahoy JD, B Emery, A Kaushal, LC Foo, JL Zamanian, KS Christopherson, Y Xing, JL Lubischer, PA Krieg, et al. (2008). A transcriptome database for astrocytes, neurons, and oligodendrocytes: a new resource for understanding brain development and function. *J Neurosci* 28:264–278.
 23. Wang S, D Chandler-Militello, G Lu, NS Roy, A Zielke, R Auvergne, N Stanwood, SK Nicolis, FJ Sim and SA Goldman. (2010). Prospective identification, isolation, and profiling of a telomerase expressing subpopulation of human neural stem cells, using sox2 enhancer-directed FACS. *J Neurosci* 30:14635.
 24. Sim FJ, HM Keyoung, JE Goldman, DK Kim, HW Jung, NS Roy and SA Goldman. (2006). Neurocytoma is a tumor of adult neuronal progenitor cells. *J Neurosci* 26:12544–12555.
 25. Hall PE, JD Lathia, NG Miller, MA Caldwell and C French-Constant. (2006). Integrins are markers of human neural stem cells. *Stem Cells* 24:2078–2084.
 26. Wright LS, J Li, MA Caldwell, K Wallace, JA Johnson and CN Svendsen. (2003). Gene expression in human neural stem cells: effects of leukemia inhibitory factor. *J Neurochem* 86:179–195.
 27. McMillan DR, KM Kayes-Wandover, JA Richardson and PC White. (2002). Very large G protein-coupled receptor-1, the largest known cell surface protein, is highly expressed in the developing central nervous system. *J Biol Chem* 277:785–792.
 28. Kim S, SH Kim, H Kim, AY Chung, YI Cha, CH Kim, TL Huh and HC Park. (2008). Frizzled 8a function is required for oligodendrocyte development in the zebrafish spinal cord. *Dev Dyn* 237:3324–3331.
 29. Cui QL, G Fragoso, VE Miron, PJ Darlington, WE Mushynski, J Antel and G Almazan. (2010). Response of human oligodendrocyte progenitors to growth factors and axon signals. *J Neuropathol Exp Neurol* 69:930–944.
 30. Nunes MC, NS Roy, HM Keyoung, RR Goodman, G McKhann, 2nd, L Jiang, J Kang, M Nedergaard and SA Goldman. (2003). Identification and isolation of multipotential neural progenitor cells from the subcortical white matter of the adult human brain. *Nat Med* 9:439–447.
 31. Singh SK, C Hawkins, ID Clarke, JA Squire, J Bayani, T Hide, RM Henkelman, MD Cusimano and PB Dirks. (2004). Identification of human brain tumour initiating cells. *Nature* 432:396–401.
 32. Callihan P, NC Zitomer, MV Stoeling, PC Kennedy, KR Lynch, RT Riley and SB Hooks. (2012). Distinct generation, pharmacology, and distribution of sphingosine 1-phosphate and dihydrosphingosine 1-phosphate in human neural progenitor cells. *Neuropharmacology* 62:988–996.

Address correspondence to:

Dr. Fraser J. Sim

Department of Pharmacology and Toxicology

School of Medicine and Biomedical Sciences

University at Buffalo

3435 Main Street

Buffalo, NY 14214

E-mail: fjsim@buffalo.edu

Received for publication January 2, 2013

Accepted after revision March 13, 2013

Prepublished on Liebert Instant Online March 14, 2013